

Electronic Supplementary Information

Simple Pyridine Hydrochlorides as Bifunctional Electron Injection and Transport Materials for High-Performance All-Solution-Processed Organic Light Emitting Diodes

Xiaojun Yin,^a Guohua Xie,^a Tao Zhou,^a Yepeng Xiang,^a Kailong Wu,^a Jingui Qin^a and Chuluo Yang,^{a,b*}

^aHubei Collaborative Innovation Center for Advanced Organic Chemical Materials, Hubei Key Lab on Organic and Polymeric Optoelectronic Materials, Department of Chemistry, Wuhan University, Wuhan, 430072, P. R. China.

^bNew Materials Technology Institute, Co-Innovation Center for Micro/Nano Optoelectronic Materials and Devices, Chongqing University of Arts and Sciences, Chongqing 402160, China

*clyang@whu.edu.cn

General Information	2
Device Fabrication and Performance Measurement	2
Materials Preparation	3
Scheme S1. Synthetic routes of the pyridine-containing precursors.....	5
Scheme S2 Synthetic routes and chemical structures of the pyridine hydrochlorides.....	6
Figure S1. TGA curves of the pyridine-containing precursors.....	7
Figure S2. DSC curves of the pyridine-containing precursors.....	8
Figure S3. The TGA curves of the PHs.....	8
Figure S4. Normalized UV-vis absorption and PL spectra of the compounds.....	9
Figure S5. Time-resolved PL signal of the different samples.....	9
Table S1. Comparison of the excitation lifetimes of the films.....	10
Figure S6-S12 ¹ H-NMR of the compounds.....	11-14
Electroluminescent properties	14

General Information

^1H NMR and ^{13}C NMR spectra were recorded on a MERCURY-VX300 spectrometer with CDCl_3 , CD_3OD or CD_2Cl_2 as the solvent, and tetramethylsilane as an internal reference. EI-MS were measured on ZAB 3F-HF Mass spectrometer. Elemental analyses of the carbon, hydrogen, and nitrogen content were carried out on a Vario EL-III microanalyzer. UV-Vis absorption spectra were recorded on a Shimadzu UV-2500 recording spectrophotometer. Photoluminescence (PL) spectra were recorded on a Hitachi F-4600 fluorescence spectrophotometer. Thermogravimetric analysis (TGA) was undertaken with a NETZSCH STA 449C instrument. The thermal decomposition temperature of the samples were determined by measuring their weight loss under a nitrogen atmosphere at a heating rate of $10\text{ }^\circ\text{C min}^{-1}$ from room temperature to $800\text{ }^\circ\text{C}$. Differential scanning calorimetry (DSC) measurements were performed on NETZSCH DSC 200 PC unit under a heating rate of $10\text{ }^\circ\text{C min}^{-1}$ from -60 to $350\text{ }^\circ\text{C}$, and their glass transition temperature (T_g) were determined from the second heating scan. Cyclic voltammetric studies of the compounds in reduction processes were carried out in nitrogen-purged dimethyl formamide (DMF) and acetonitrile solution at room temperature with a CHI voltammetric analyzer. The Bu_4NPF_6 (0.1 M) was employed as the supporting electrolyte, and ferrocenium-ferrocene (Fc/Fc^+) was served as the internal standard. The conventional three-electrode configuration consists of a platinum working electrode, a platinum wire counter electrode, and a silver/silver chloride (Ag/Ag^+) reference electrode. The LUMO energy levels (eV) of these compounds were calculated according to the formula: $- [4.8\text{ eV} + (E_{\text{onset, reversible}} - E_{1/2(\text{Fc}/\text{Fc}^+)})]$. The PL lifetimes was measured by a single photon counting spectrometer from Edinburgh Instruments (FLS920) with a Picosecond Pulsed UV-LASTER (LASTER377) as the excitation source.

Device Fabrication and Performance Measurement

The patterned ITO coated glasses were undergone ultrasonic cleaning consecutively in acetone and ethanol. After UV-ozone treatment, a 30 nm-thick PEDOT:PSS (CLEVIOS P VP Al 4083) used as a hole-injecting layer was spin-coated on the ITO substrate and then dried in the glove-box at $120\text{ }^\circ\text{C}$ for 10 min. The emissive layer (EML) was spin-coated on the top of the PEDOT: PSS layer from chlorobenzene solution. The thickness of the EML was about 80 nm. And then electron transporting layer was spin-coated atop the EML. Finally, a composite cathode composed of Ba (20 nm) and Al (200 nm) was evaporated through a shadow mask.

The current density–voltage–luminance characteristics were measured combining a Keithley 2400 source measurement unit and Spectroscan spectrometer PR735. The external quantum efficiency was calculated by assuming a Lambertian emission profile.

Materials Preparation

All reagents commercially available were used as received unless otherwise indicated. Solvents were purified according to standard procedures. The starting material of 2,3,5-tribromopyridine,^[1] 2-(3-(4,4,5,5-tetramethyl-1,3,2-dioxaborolan-2-yl)phenyl)pyridine, 3-(3-(4,4,5,5-tetramethyl-1,3,2-dioxaborolan-2-yl)phenyl)pyridine, 4-(3-(4,4,5,5-tetramethyl-1,3,2-dioxaborolan-2-yl)phenyl)pyridine,^[2] and 1,4-bis(4,4,5,5-tetramethyl-1,3,2-dioxaborolan-2-yl)benzene^[3] were synthesized according to the literature procedures. The pyridine-based precursor of 3,3'-(5'-(3-(pyridin-3-yl)phenyl)-[1,1':3',1''-terphenyl]-3,3''-diyl)dipyridine (TmPyPB) were commercially available.

Synthesis of 1,4-bis(3,5-dibromopyridin-2-yl)benzene (1) : A mixture of 2,3,5-tribromopyridine (2.04 g, 6.45 mmol), 1,4-bis(4,4,5,5-tetramethyl-1,3,2-dioxaborolan-2-yl)benzene (851 mg, 2.57 mmol), Pd(OAc)₂ (132 mg), PPh₃ (312 mg) and potassium carbonate (1.78 g) in 40 ml degassed acetonitrile and 20 ml methanol was stirred at 50 °C for 24 h under an argon atmosphere. After cooling to room temperature, the precipitate was filtered and washed with distilled water, methanol and dichloromethane successively. The remaining solid was dried in vacuum to yield a light yellow powder (0.85 g, yield: 62%). ¹H NMR (300 MHz, CDCl₃) δ [ppm]: 8.70 (s, 2H), 8.18 (s, 2H), 7.78 (s, 4H); MS (EI): *m/z* 547.8 [M⁺]. Anal. calcd for C₁₆H₈Br₄N₂ (%): C 35.08, H 1.47, N 5.11; found: C 34.82, H 1.54, N 5.03.

Synthesis of Tm2PyDPB: To a mixture of Compound 1 (655 mg, 1.19 mmol), 2-(3-(4,4,5,5-tetramethyl-1,3,2-dioxaborolan-2-yl)phenyl)pyridine (2.3 g, 8.2 mmol), potassium carbonate (2 g) and Pd(PPh₃)₄ (50 mg) was added 70 ml of degassed dioxane. The suspension was stirred at 100 °C for 2~3 d. After cooling to room temperature, the mixture was poured into water and then extracted with dichloromethane (50 ml × 3). The combined organic phase was washed with brine and water, and then dried over anhydrous Na₂SO₄. After the solvent had been removed under reduced pressure, the residue was purified by column chromatography on

silica gel using dichloromethane/methanol 40:1 (v/v) as the eluent to give a white solid (865 mg, yield: 86%). ¹H NMR (300 MHz, CDCl₃) δ [ppm]: 9.02 (s, 2H), 8.73 (d, *J* = 4.2 Hz, 2H), 8.67 (d, *J* = 3.9 Hz, 2H), 8.31 (s, 2H), 8.09 (s, 2H), 8.05 (d, *J* = 7.5 Hz, 2H), 7.98 (s, 2H), 7.89 (d, *J* = 7.8 Hz, 2H), 7.71-7.81(m, 8H), 7.62 (t, *J* = 7.8 Hz, 4H), 7.42 (s, 4H), 7.15-7.29 (m, 8H); ¹³C NMR (75 MHz, CDCl₃) δ [ppm]: 157.03, 155.74, 149.97, 147.13, 140.52, 140.04, 139.56, 138.04, 137.34, 137.11, 136.18, 135.20, 130.67, 130.08, 129.83, 129.01, 127.91, 126.98, 126.28, 125.97, 122.71, 120.96; MS (EI): *m/z* 844.7 [M⁺]. Anal. calcd for C₆₀H₄₀N₆ (%): C 85.28, H 4.77, N 9.95; found: C 85.27, H 4.88, N 10.05.

Synthesis of Tm3PyDPB : Following the same procedure of Tm2PyDPB, using 3-(3-(4,4,5,5-tetramethyl-1,3,2-dioxaborolan-2-yl)phenyl)pyridine as the precursor to give the target compound of Tm3PyDPB as a white solid (yield 63%). ¹H NMR (300 MHz, CDCl₃) δ [ppm]: 9.01 (s, 2H), 8.91 (s, 2H), 8.72 (s, 2H), 8.64 (d, *J* = 3.3 Hz, 2H), 8.57 (d, *J* = 3.9 Hz, 2H), 8.01 (s, 2H), 7.97 (d, *J* = 5.4 Hz, 2H), 7.93 (s, 2H), 7.63-7.72 (m, 8H), 7.49 (s, 4H), 7.37-7.42 (m, 8H), 7.31-7.35 (m, 4H); ¹³C NMR (75 MHz, CDCl₃) δ [ppm]: 155.75, 148.92, 148.72, 148.44, 148.24, 147.06, 140.50, 139.41, 138.98, 138.25, 137.04, 136.26, 136.14, 135.75, 134.93, 134.92, 130.01, 129.87, 129.34, 128.38, 127.17, 126.94, 126.32, 126.04, 123.68; MS (EI): *m/z* 844.1 [M⁺]. Anal. calcd for C₆₀H₄₀N₆ (%): C 85.28, H 4.77, N 9.95; found: C 85.64, H 4.61, N 9.75.

Synthesis of Tm4PyDPB : Following the same procedure of Tm2PyDPB, using 4-(3-(4,4,5,5-tetramethyl-1,3,2-dioxaborolan-2-yl)phenyl)pyridine as the precursor to give the target compound of Tm4PyDPB as a white solid (yield 62%). ¹H NMR (300 MHz, CDCl₃) δ [ppm]: 9.01 (s, 2H), 8.71 (d, *J* = 3.3 Hz, 4H), 8.62 (d, *J* = 3.9 Hz, 4H), 8.00 (s, 2H), 7.90 (s, 2H), 7.68-7.77 (m, 14H), 7.43 (s, 4H), 7.33-7.38 (m, 8H); ¹³C NMR (75 MHz, CDCl₃) δ [ppm]: 155.81, 150.35, 147.85, 147.71, 147.09, 140.34, 139.44, 139.27, 138.45, 138.20, 136.90, 135.55, 134.91, 130.15, 130.03, 129.90, 129.36, 128.32, 127.84, 127.00, 126.21, 125.82, 121.77, 121.65; MS (EI): *m/z* 843.5 [M⁺]. Anal. calcd for C₆₀H₄₀N₆ (%): C 85.28, H 4.77, N 9.95; found: C 85.34, H 4.82, N 9.94.

General Procedure for Hydrochloric Acid-treatment Reaction : To a 50 ml round-bottom flask was added concentrated hydrochloric acid (20 ~ 30 ml) and the pyridine-containing precursors (TmPyPB, Tm2PyDPB, Tm3PyDPB or Tm4PyDPB, 1 mmol). The mixture was allowed to stir at room temperature for about 6~8 h. The light yellow liquid was then heated to about 80 °C and distilled under reduced pressure to remove the residual hydrochloric acid.

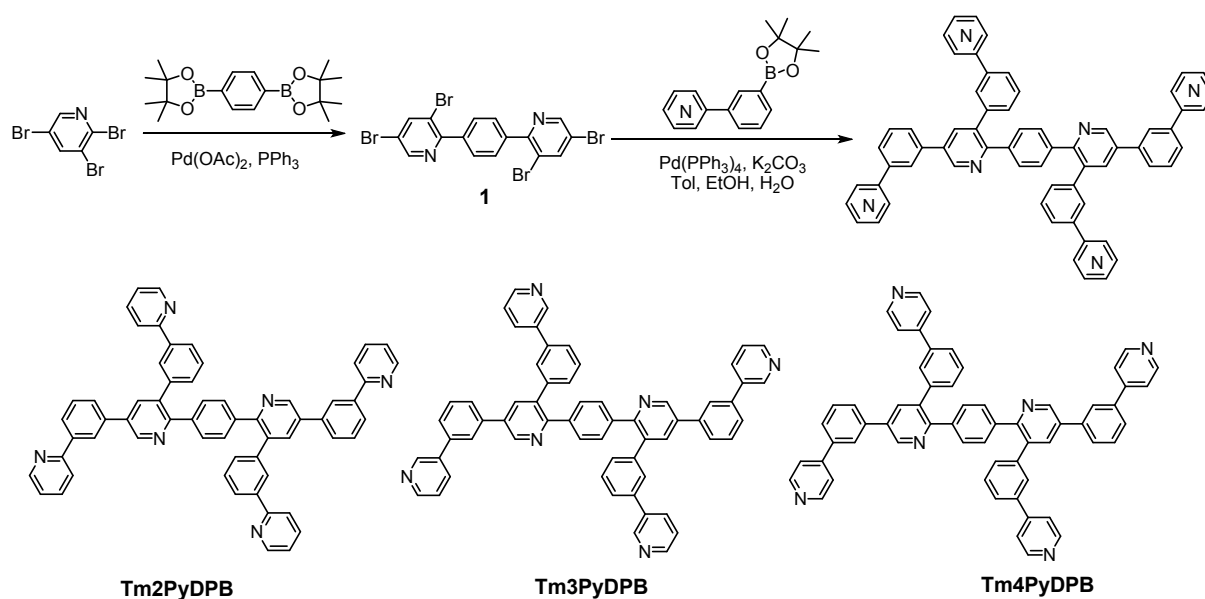
The residue was dissolved in ethanol, then precipitated by n-hexane to give the pyridine hydrochlorides with almost quantitative conversion.

PH-1 : ^1H NMR (300 MHz, CD_3OD) δ [ppm]: 9.35 (s, 3H), 9.07 (d, $J = 8.7$ Hz, 3H), 8.87 (d, $J = 8.7$ Hz, 3H), 8.30 (s, 3H), 8.21-8.16 (m, 6H), 8.08 (d, $J = 6.6$ Hz, 3H), 7.90 (d, $J = 7.2$ Hz, 3H), 7.77 (t, $J = 7.2$ Hz, 3H), 4.91 (s, 3H); Anal. Calcd for $\text{C}_{39}\text{H}_{27}\text{N}_3 \cdot 3\text{HCl}$ (%): Cl 16.44; found 16.23.

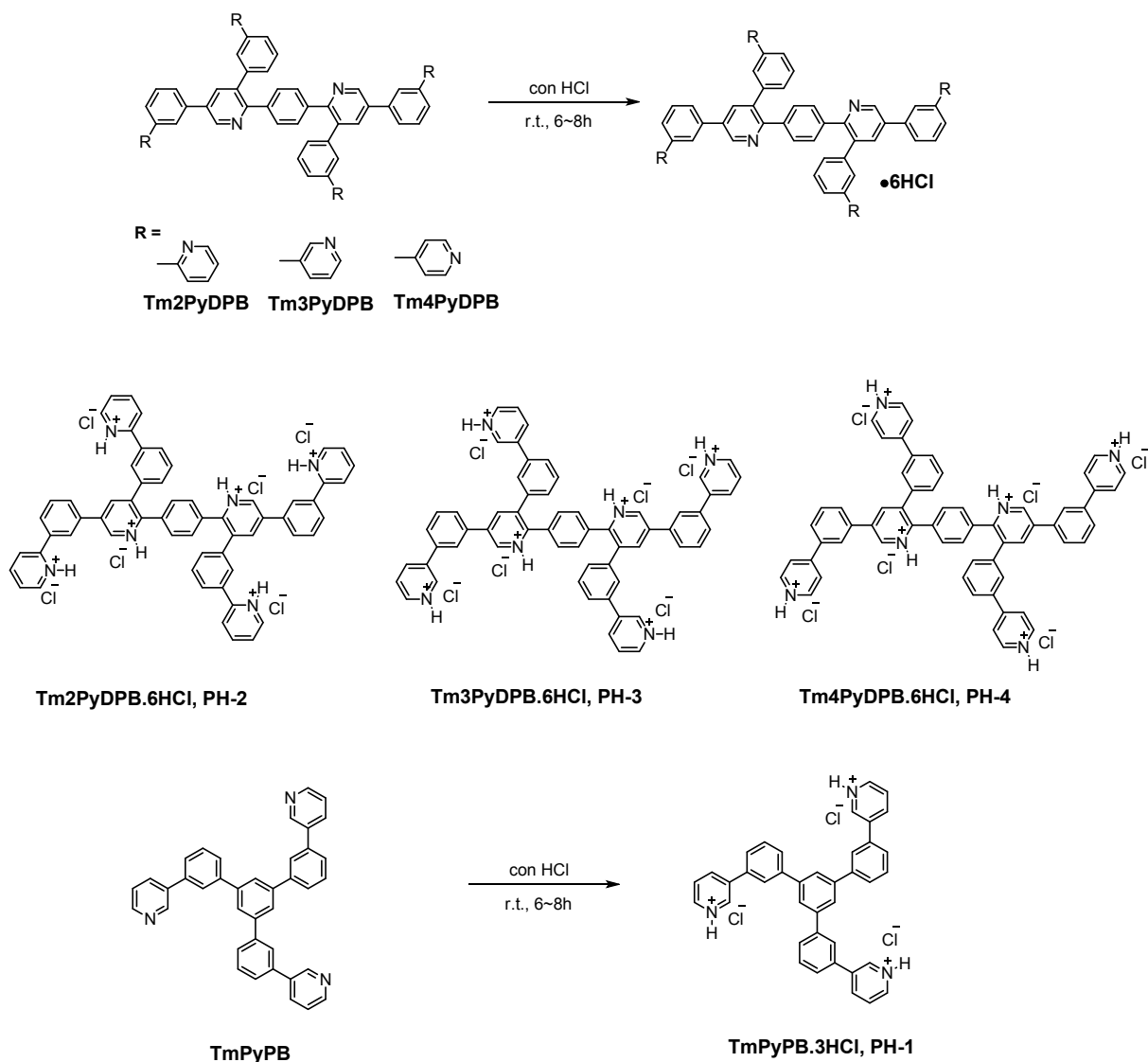
PH-2: ^1H NMR (300 MHz, CD_3OD) δ [ppm]: 9.32 (s, 2H), 9.08 (s, 2H), 8.93 (br, 4H), 8.73-8.64 (m, 8H), 8.46-8.40 (m, 4H), 8.33 (d, $J = 7.5$ Hz, 2H), 8.17-8.07 (m, 8H), 7.93 (t, $J = 7.5$ Hz, 2H), 7.61 (br, 6H), 7.45 (d, $J = 3.3$ Hz, 2H), 4.91 (m, 6H) Anal. Calcd for $\text{C}_{60}\text{H}_{40}\text{N}_6 \cdot 6\text{HCl}$ (%): Cl 20.00; found 20.12.

PH-3: ^1H NMR (300 MHz, CD_3OD) δ [ppm]: 9.44 (s, 2H), 9.33 (br, 2H), 9.26 (br, 2H), 9.17 (br, 2H), 8.98-8.89 (m, 8H), 8.51 (br, 2H), 8.24-8.12 (m, 8H), 8.05 (d, $J = 7.2$ Hz, 2H), 7.92-7.83 (m, 4H), 7.64 (br, 4H), 7.54 (t, $J = 5.7$ Hz, 2H), 7.43 (t, $J = 4.5$ Hz, 2H), 4.92 (m, 6H); Anal. Calcd for $\text{C}_{60}\text{H}_{40}\text{N}_6 \cdot 6\text{HCl}$ (%): Cl 20.00; found 19.68.

PH-4: ^1H NMR (300 MHz, CD_3OD) δ [ppm]: 9.37 (s, 2H), 9.02 (s, 2H), 8.95-8.93 (m, 8H), 8.66 (d, $J = 3.9$ Hz, 6H), 8.46 (br, 4H), 8.28-8.19 (m, 6H), 8.07 (br, 2H), 7.93-7.89 (m, 2H), 7.67-7.52 (m, 8H), 4.88 (m, 6H); Anal. Calcd for $\text{C}_{60}\text{H}_{40}\text{N}_6 \cdot 6\text{HCl}$ (%): Cl 20.00; found 20.21.



Scheme S1. Synthetic routes of the pyridine-containing precursors.



Scheme S2 Synthetic routes and chemical structures of the pyridine hydrochlorides.

General procedure for precipitation titration method

The chlorinity of the pyridine hydrochlorides were quantified by precipitation titration method. Firstly, 10~20 mg pyridine hydrochlorides (PH-1, PH-2, PH-3 or PH-4) was dissolved in 10 ml deionized water, then excessive amounts of AgNO_3 standard solution (0.06434 mol/L, calibrated by NaCl standard solution) was added to insure the chloridion could be precipitated completely. After stirred at room temperature for 30 min, the suspension was concentrated to about 5 ml *via* evaporation. The excess AgNO_3 was back-titrated by NH_4SCN standard solution (0.02995 mol/L, calibrated by AgNO_3 standard solution), and the indicator was

Fe(NO₃)₃ solution. According to the following formula, the content of Cl and the unknown x can be accurately calculated.

$$\text{Cl (\%)} = \frac{(c_{Ag(NO_3)}V_{Ag(NO_3)} - c_{NH_4SCN}V_{NH_4SCN}) \times M_{Cl} \times 100}{m} = \frac{x \times M_{Cl}}{M + x \times M_{HCl}}$$

Where x is the numbers of HCl in PHs:

Herein TmPyPB· x HCl representative PH-1, and the calculated x is 3;

Tm2PyDPB· x HCl representative PH-2, and the calculated x is 6;

Tm3PyDPB· x HCl representative PH-3, and the calculated x is 6;

Tm4PyDPB· x HCl representative PH-4, and the calculated x is 6.

Thermodynamic Property

The good thermal stabilities of the pyridine-based precursors were revealed by their high decomposition temperatures (T_{d5}) in the thermogravimetric analysis (Figure S1) and high glass transition temperatures (T_g s) from differential scanning calorimetry (Figure S2), and the detailed data were presented at Table S1. The thermodynamic properties of these PHs are displayed in Figure S3.

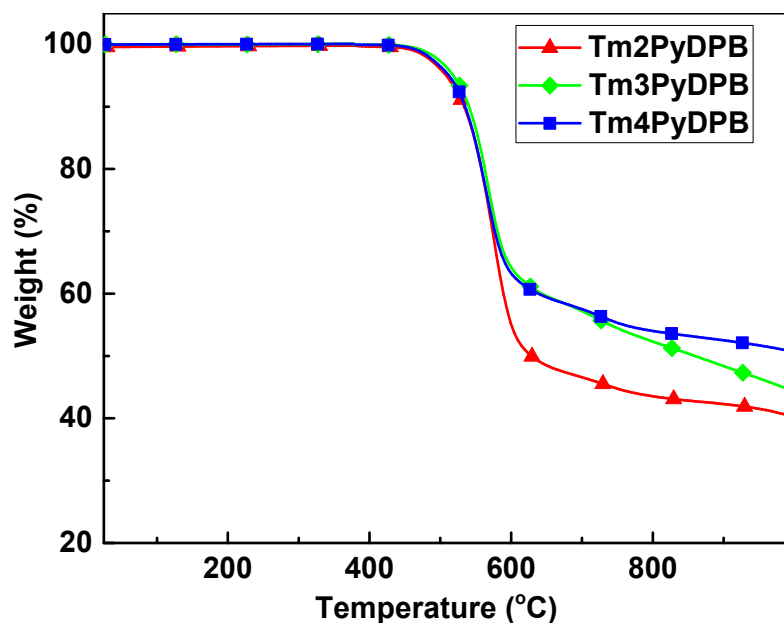


Figure S1. TGA curves of the pyridine-containing precursors.

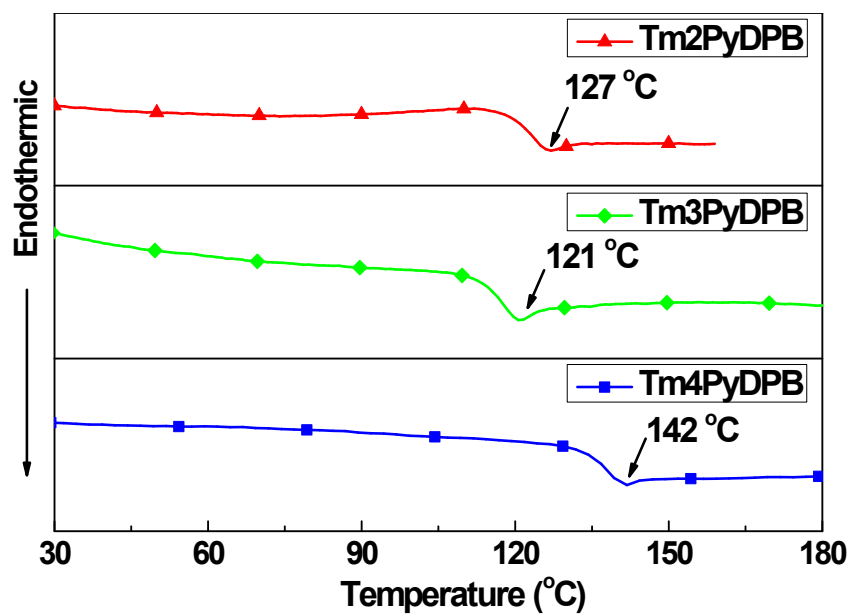


Figure S2. DSC curves of the pyridine-containing precursors.

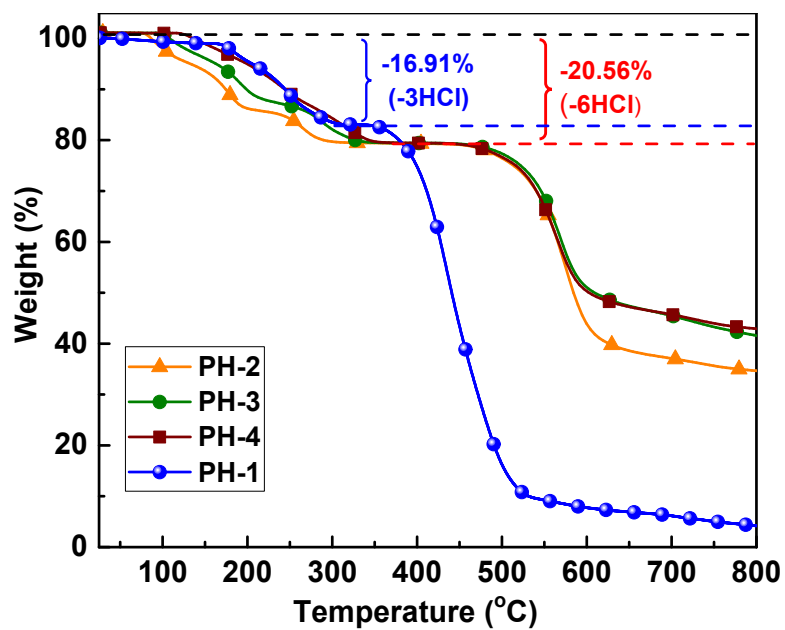


Figure S3. The TGA curves of the PHs.

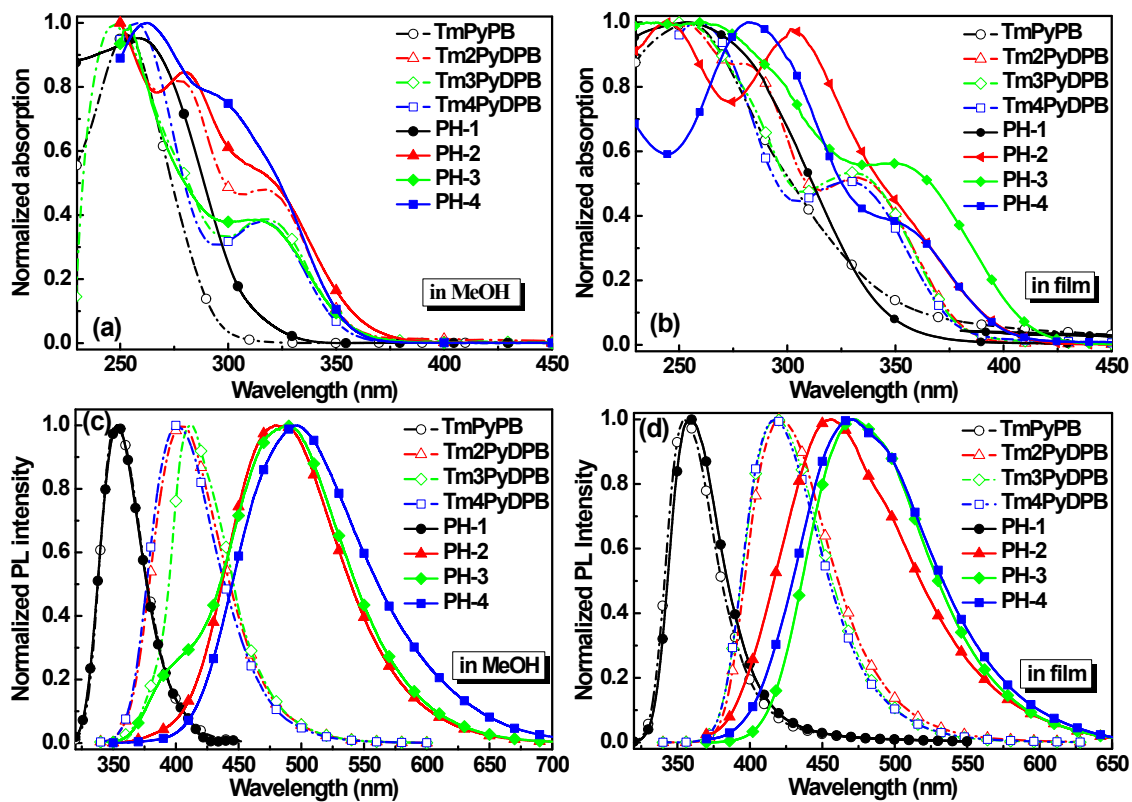


Figure S4. Normalized UV-vis absorption in methanol (a) and in film (b), and PL spectra in methanol (c) and in film (d) of the compounds.

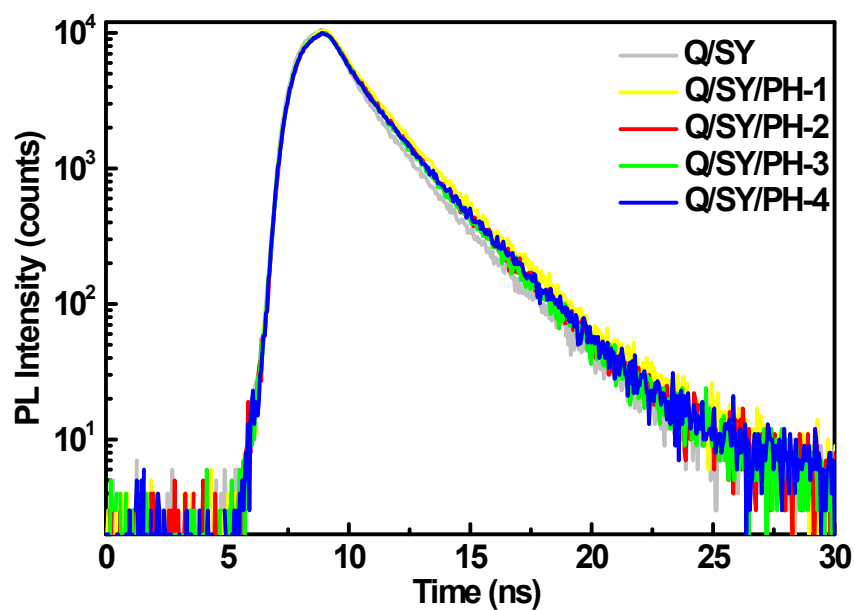
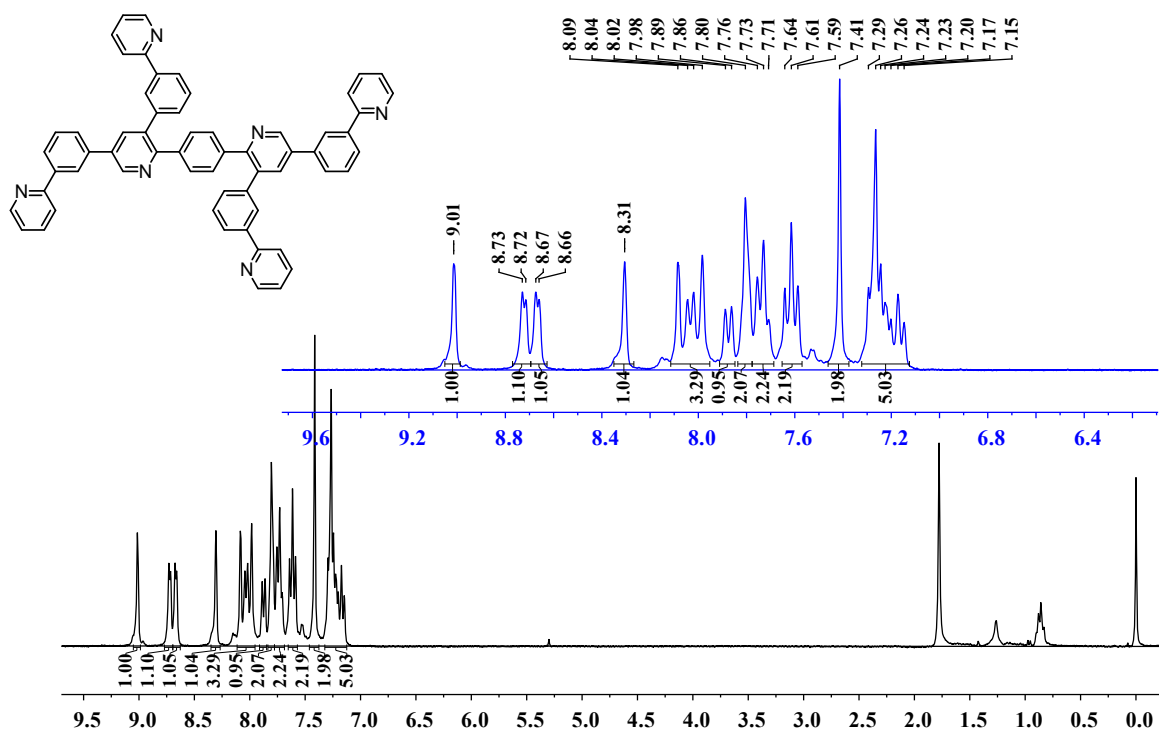
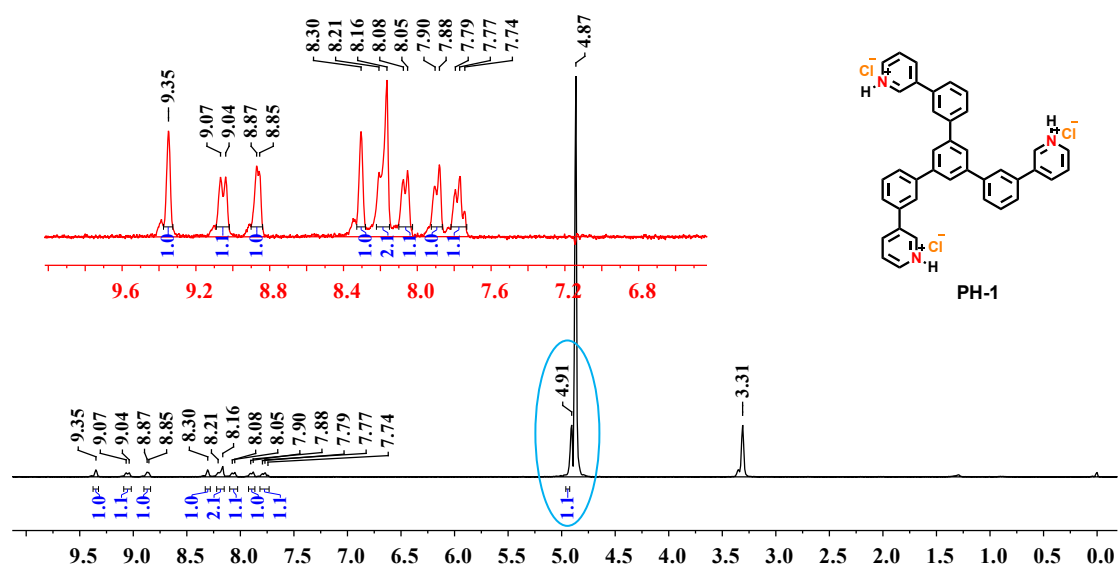


Figure S5. Time-resolved PL signal of the different samples on quartz/PEDOT:PSS substrates.

Table S1. Comparison of the excitation lifetimes of the films.

sample	$\tau_1 (f_1)$ [ns]	$\tau_2 (f_2)$ [ns]	χ^2	τ_{avt} [ns]
quartz/PEDOT:PSS/SY	1.24 (0.45)	2.60 (0.55)	1.12	1.99
quartz/PEDOT:PSS/SY/PH-1	1.55 (0.50)	2.83 (0.50)	1.29	2.19
quartz/PEDOT:PSS/SY/PH-2	1.44 (0.48)	2.70 (0.52)	1.15	2.10
quartz/PEDOT:PSS/SY/PH-3	1.35 (0.42)	2.58 (0.58)	1.15	2.06
quartz/PEDOT:PSS/SY/PH-4	1.37 (0.39)	2.62 (0.61)	1.16	2.13

H-NMR spectra of the pyridine-containing precursors and their corresponding Pyridine Hydrochlorides.



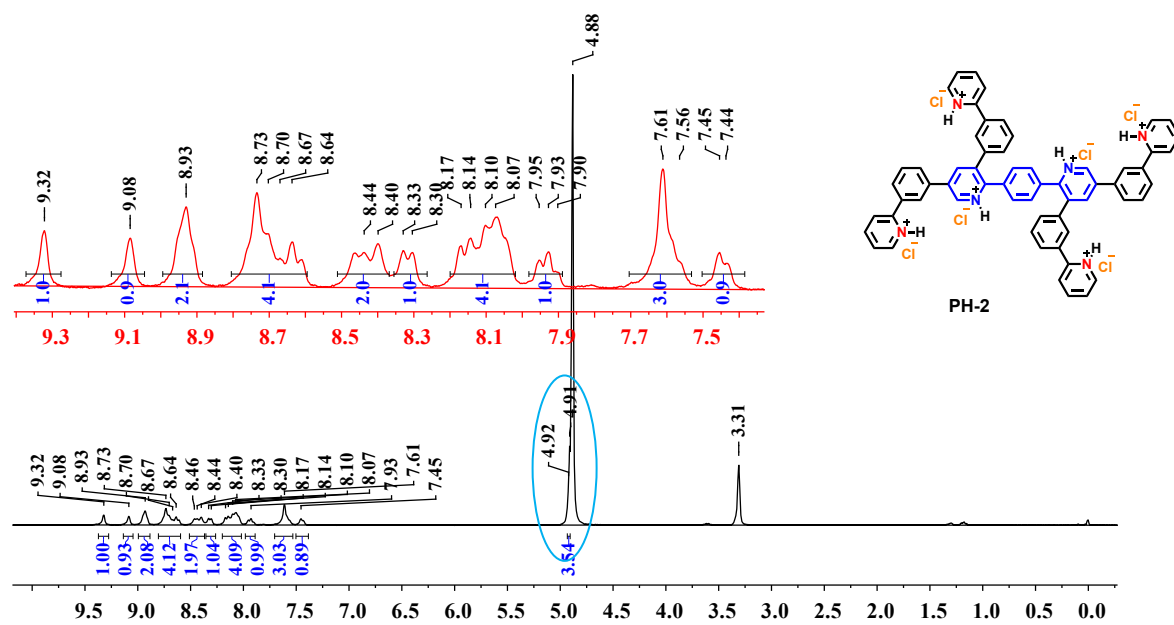


Figure S8 ¹H-NMR of PH-2 in CD₃OD.

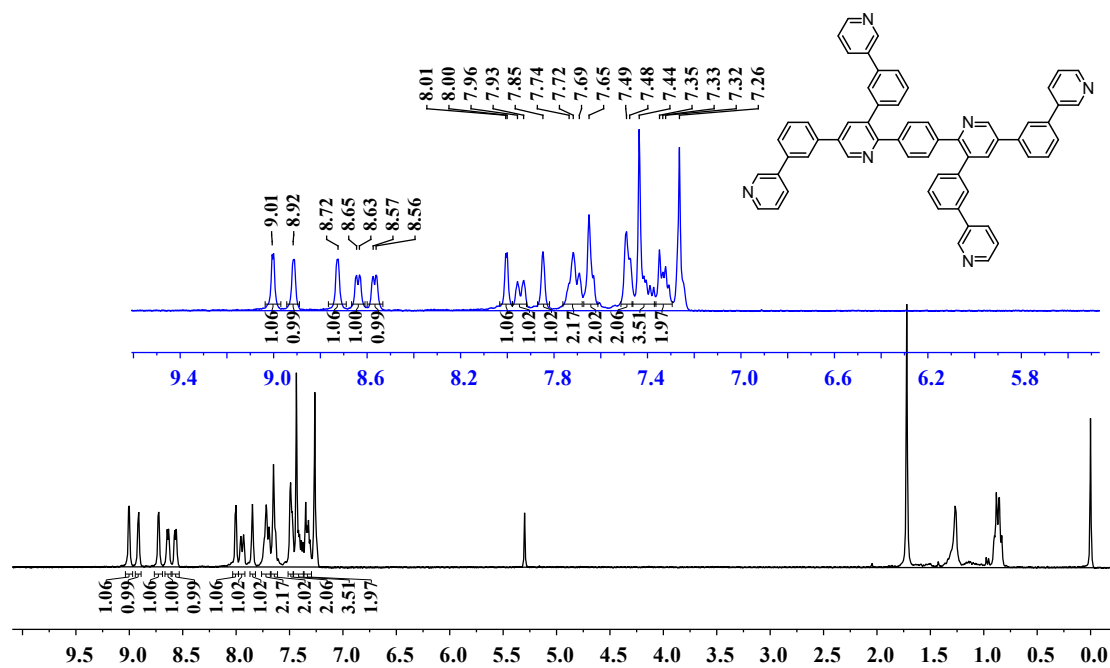


Figure S9 ¹H-NMR of Tm₃PyDPB in CDCl₃.

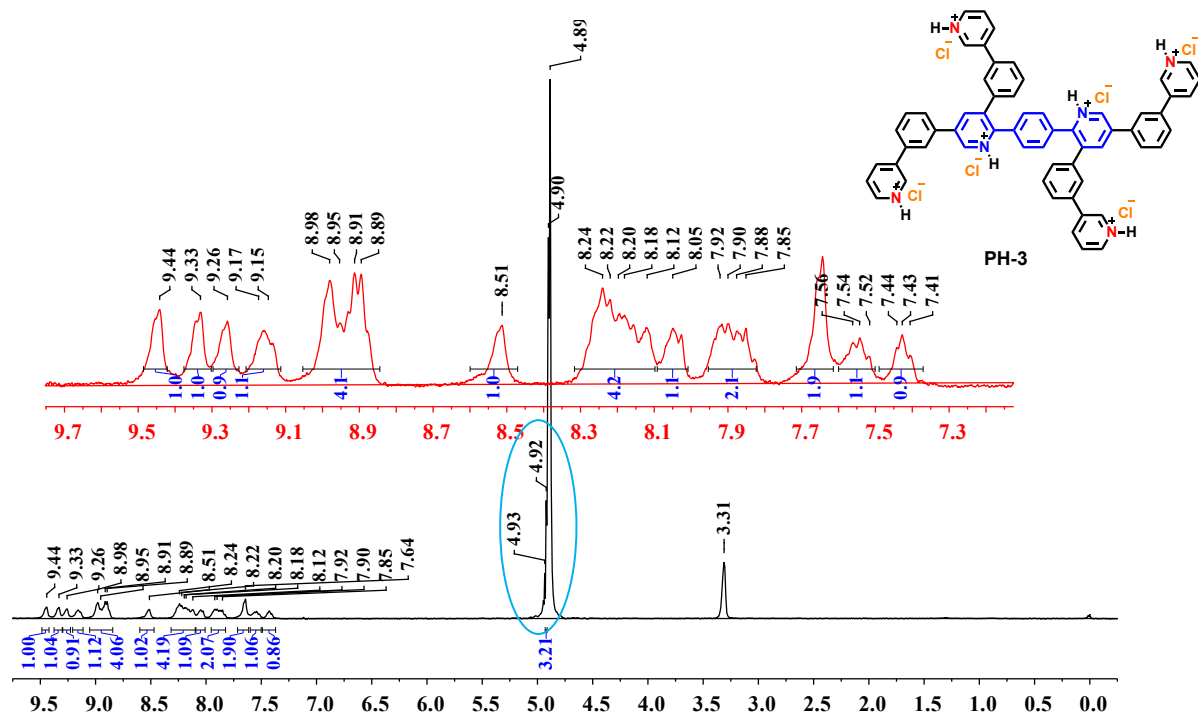


Figure S10 $^1\text{H-NMR}$ of PH-3 in CD_3OD .

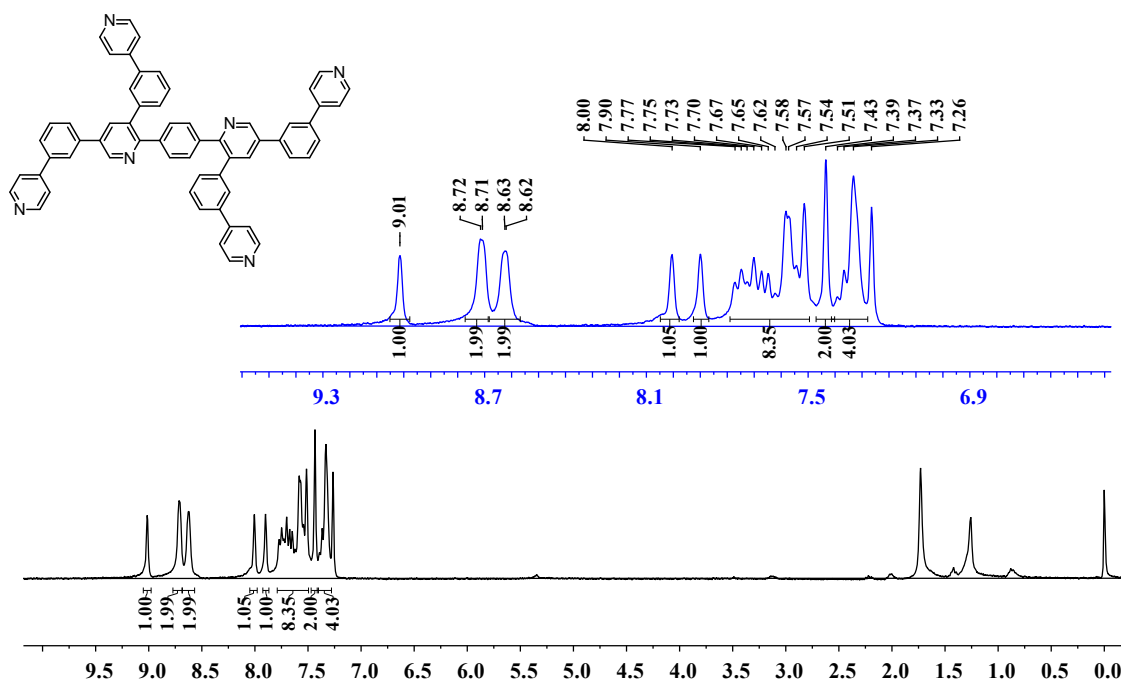


Figure S11 $^1\text{H-NMR}$ of Tm4PyDPB in CDCl_3 .

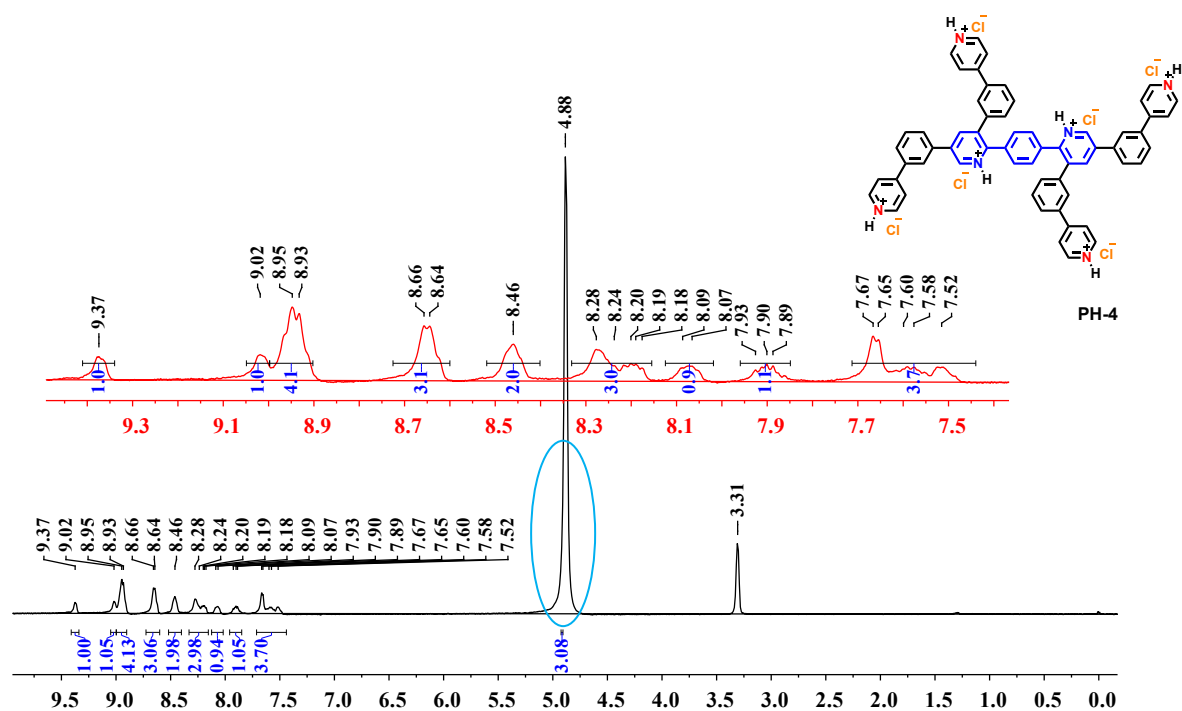


Figure S12 $^1\text{H-NMR}$ of PH-4 in CD_3OD .

Electroluminescent properties.

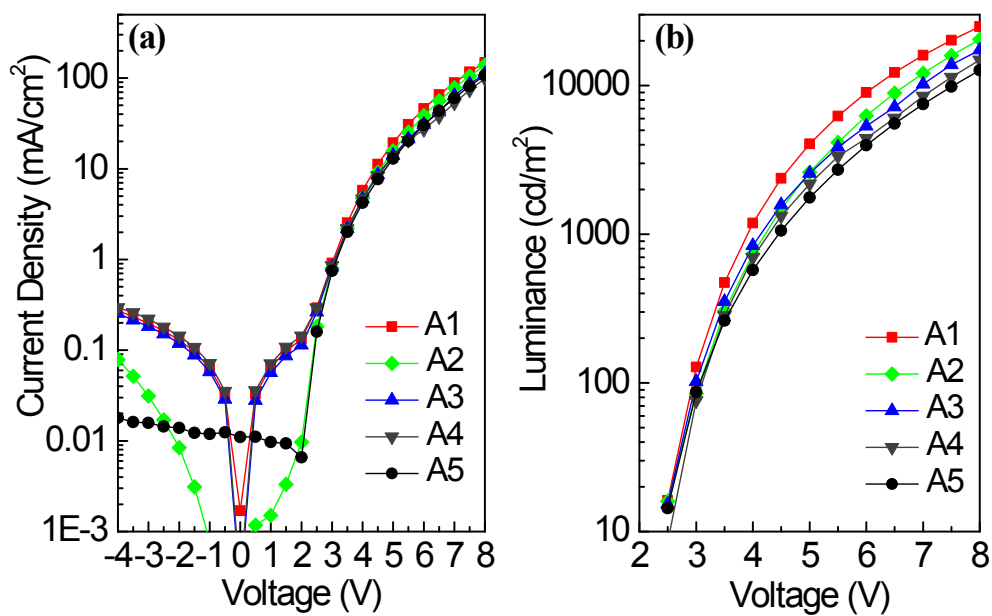


Figure S13. Current density (a) and luminance (b) *versus* voltage curves of Device A1~A5.

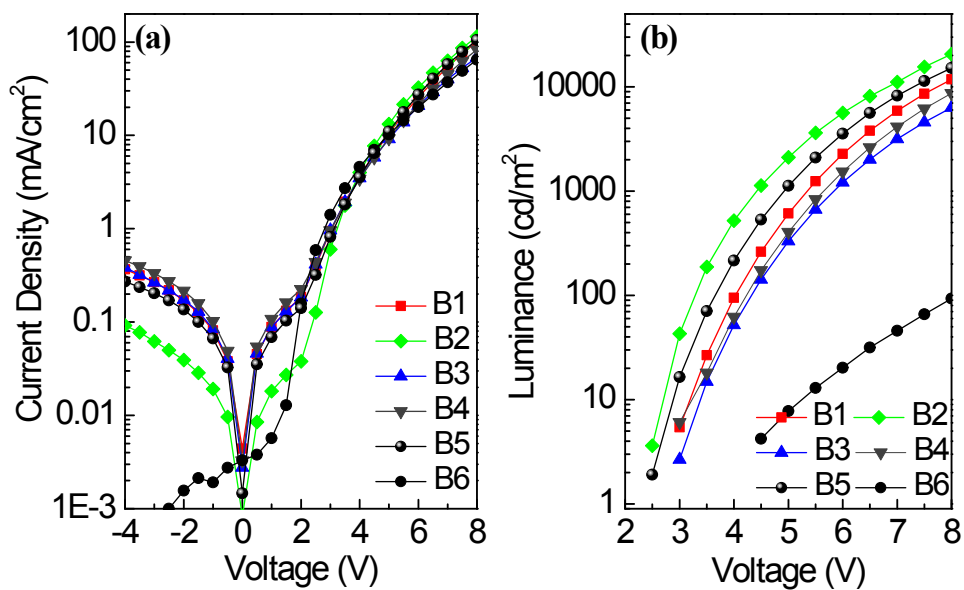


Figure S14. Current density (a) and luminance (b) *versus* voltage curves of Device B1~B6.

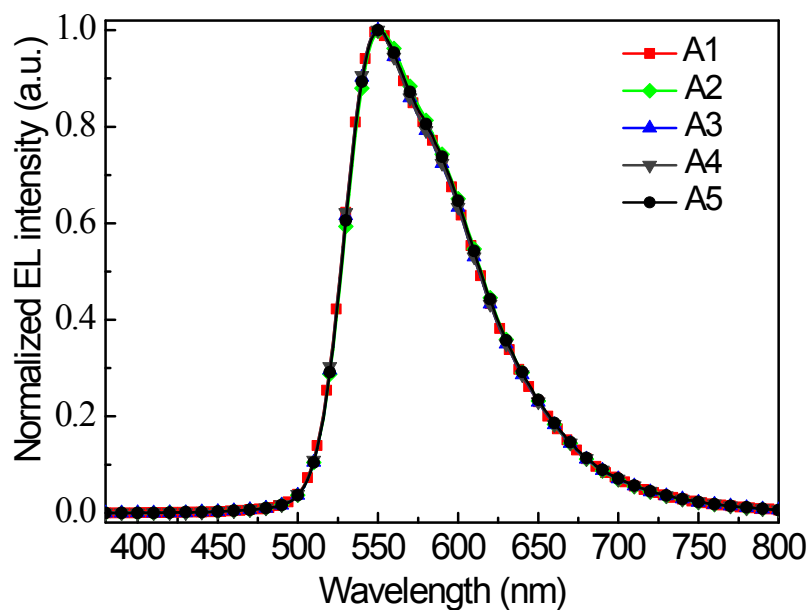


Figure S15. Normalized electroluminescence spectra of Device A1~A5 at 2 mA cm^{-2}

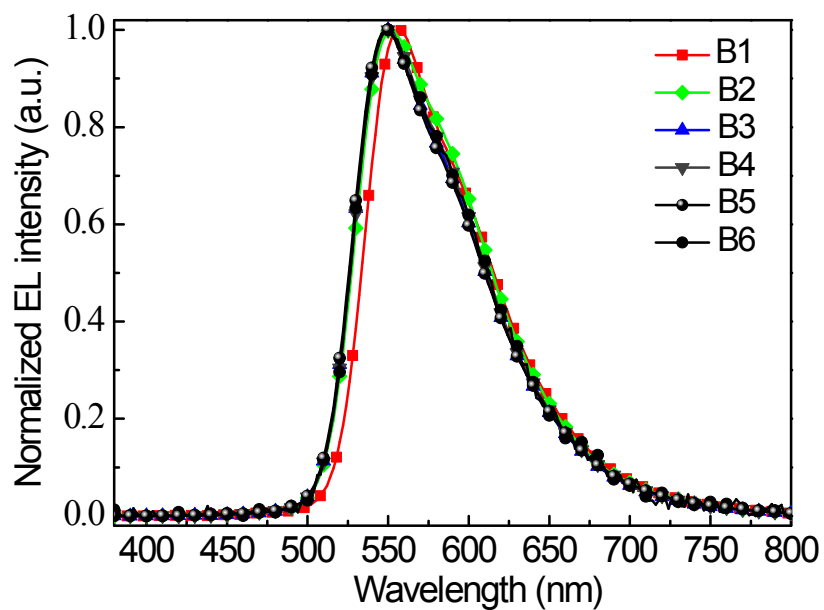


Figure S16. Normalized electroluminescent spectra of Device B1~B6 at 2 mA cm^{-2}

- [1] S. Rault, G. Burzicki, A. Voisin-Chiret, J. Santos, *Synthesis* **2010**, 2010, 2804.
- [2] S.-J. Su, Y. Takahashi, T. Chiba, T. Takeda, J. Kido, *Adv. Funct. Mater.* **2009**, 19, 1260.
- [3] A. Britze, J. Jacob, V. Choudhary, V. Moellmann, G. Grundmeier, H. Luftmann, D. Kuckling, *Polymer* **2010**, 51, 5294.